

A BRINE MODULE FOR TOUGH2 - EXAMPLES

W. M. KISSLING

Applied Mathematics, Industrial Research Limited, Lower Hutt, NZ

SUMMARY – This paper presents a number of examples of the use of the simulation code NaCL-TOUGH2. These examples demonstrate that the code can handle flows of high temperature and pressure hypersaline brines and accompanying phase changes between liquid, vapour and solid phases in simple physical problems. A 2D TVZ-like problem is also presented which is the first application of the code to a problem of geophysical interest.

1. INTRODUCTION

The geothermal fluids in the TVZ are H_2O -NaCl mixtures (brines) with typical surface concentrations of about 1000 ppm. The concentration is probably much higher near the heat source, where the NaCl is formed through the reaction of magmatic HCl with sodium bearing minerals (feldspars) in the country rock (e.g. Giggenbach, 1992). Thus, NaCl is formed at depth and provides an important geochemical indicator of processes occurring near the TVZ heat source. Indeed, some authors consider the phase behaviour of brines at high temperatures and pressures to be important in understanding the nature of the heat source of the TVZ geothermal fields. Christenson *et al.*, (1998) find highly saline brines (> 30% by weight) in inclusions associated with the Ngatamariki diorite intrusion and McNabb (1992) proposes a saline 'hot-plate' as the TVZ heat source.

In order to simulate these types of process in the TVZ, a new version of the TOUGH2 simulation code (NaCl-TOUGH2) has been developed. NaCl-TOUGH2 is unique because it incorporates a description of the complete phase diagram for H_2O -NaCl mixtures, including liquid, vapour and solid phases, over a wide range of pressure, temperature and concentration (PTX) conditions. There are six distinct regions (Table 1) in the phase diagram and the fluid state must be described by different primary variables in each region. There are two single-phase regions, three two-phase regions and one three-phase region. The code provides the means for modelling the movement of fluid between the regions and the consequent exchange of primary variables in response to changing PTX conditions.

Table 1. Definition of the states in H_2O -NaCl phase diagram.

State	Phases
1	Unsaturated liquid
2	Saturated liquid
3	Unsaturated two-phase
4	Saturated two-phase
5	Unsaturated vapour
6	Saturated vapour

In a previous NZ Geothermal Workshop paper (Kissling, 2000) the following features of the code were discussed in detail, and the reader is referred to that paper for more detail.

- H_2O -NaCl phase space
- Thermodynamic and transport properties of brines
- Conservation equations for water, salt, heat
- Fluid states and primary variables
- Phase changing rules

To briefly reiterate the H_2O -NaCl phase space comprises six different regions (or states). These are shown in Figure 1 (for 350 °C) and Figure 2 (for 550 °C). In these figures, the symbols l, g, s, refer to the liquid, vapour and solid phases respectively. The code can handle the transport of fluid in all of these states (Table 1), and the phase changes that are necessary as the fluid state changes between states.

For each state, a different set of primary variables is needed to describe the thermodynamic state of the fluid. For single phase fluids, these variables are the pressure (P), temperature (T) and salt mass fraction (X). For two-phase fluids the primary variables are P, T and the saturation of one of the phases, and for the three-phase surface, the primary variables are the temperature and the liquid and vapour saturations. The primary variables for each phase are summarised in Table 2.

Table 2. Primary variables for each of the six states in the H_2O -NaCl phase diagram.

State	Description	Primary Variables
1	Unsaturated liquid	P,T,X
2	Saturated liquid	P,T,S _l
3	Unsaturated Two-phase	P,T,S _l
4	Saturated Two-phase	T,S _l ,S _g
5	Unsaturated gas	P,T,X
6	Saturated gas	P,T,S _g

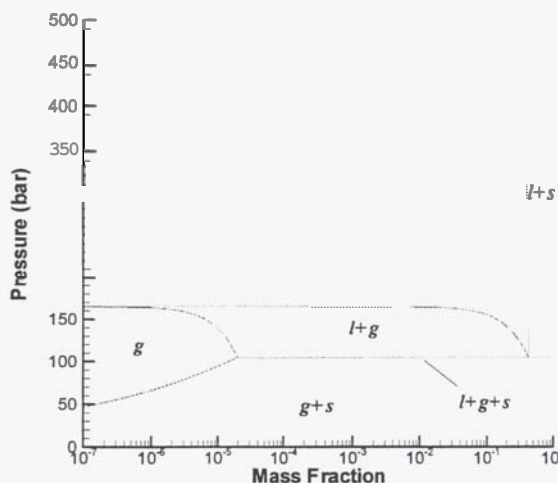


Figure 1. Phase diagram for H_2O -NaCl mixtures at 350 $^{\circ}\text{C}$. This diagram is representative of the phase behaviour for $T < 374.15$ $^{\circ}\text{C}$. Regions are labelled according to the different phases present - gas (g), liquid (l) and solid (s).

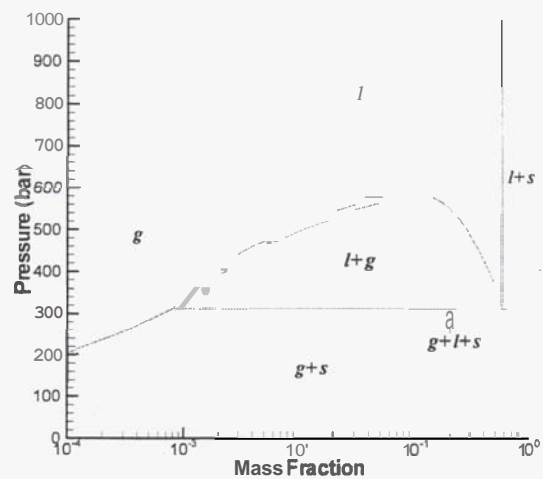


Figure 2. Phase diagram for H_2O -NaCl mixtures at 500 $^{\circ}\text{C}$. This diagram is representative of the phase behaviour between 374.15 $^{\circ}\text{C}$ and 800 $^{\circ}\text{C}$. Regions are labelled according to the different phases present - gas (g), liquid (l) and solid (s).

In this paper the emphasis is on applications of this code. Examples are presented which show that NaCl-TOUGH2 can simulate a variety flow problems involving hyper-saline brines at high temperatures and pressures. These examples show that the code can deal with complex flows involving many phase changes as well as moderately sized problems which are required for modelling the geophysical systems of interest.

2. SIMPLE PHASE CHANGES

In this section a number of simple examples are presented to illustrate that the code handles all possible phase changes which can occur at temperatures of 350 $^{\circ}\text{C}$ and 550 $^{\circ}\text{C}$. The

examples are run with a two element grid, as this has the minimum number (1) of connections permitted, and identical 'actions' are performed on each element. Symmetry ensures that identical conditions are maintained in each element. This also means that there is no flow between the elements, so the permeability is not relevant. The element volume is 10^9 m^3 and other rock properties are porosity 0.10, heat capacity 1000 J/kg/K and density 2650 kg/m^3 .

In the first example, the initial pressure, temperature and salt mass fraction are 500 bar, 350 $^{\circ}\text{C}$ and 0.3 respectively. Fluid is withdrawn from the system at 1 kg/s . Figure 3 shows the evolution of the liquid, vapour and solid saturations for this case. As the pressure drops, the fluid first boils and a vapour phase appears at approximately 4.5×10^9 s. Further fluid withdrawal reduces the pressure and at 7×10^{10} s the liquid phase disappears as the fluid enters the gas plus solid phase region of the phase diagram. Beyond about 10^{11} s, fluid withdrawal from the system is no longer possible as the pressure has essentially reached zero.

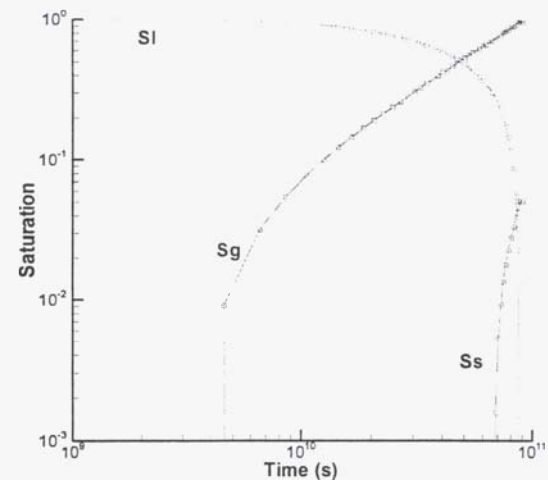


Figure 3. Evolution of liquid, vapour and solid phase saturations for a 1D 'box' of hypersaline fluid, initially at $P = 500$ bar, $T = 350$ $^{\circ}\text{C}$ and $X = 0.3$. Fluid is withdrawn from the box at the rate of 1 kg/s .

In the second example, the initial pressure, temperature and salt mass fraction are 500 bar, 550 $^{\circ}\text{C}$ and 0.5 . In this case fluid with a salinity of 0.5 is added at 0.2 kg/s , and fluid is withdrawn from the system at 0.188 kg/s . The initial fluid state is saturated liquid brine, and so solid and liquid phases are present initially. As the system evolves the pressure drops, and shortly after 10^9 s it reaches the three-phase surface, and a gas phase is created. The pressure continues to fall, and the gas and solid saturations increase, while the liquid phase finally disappears at about 8×10^{10} s. These saturation changes are shown in Figure 4.

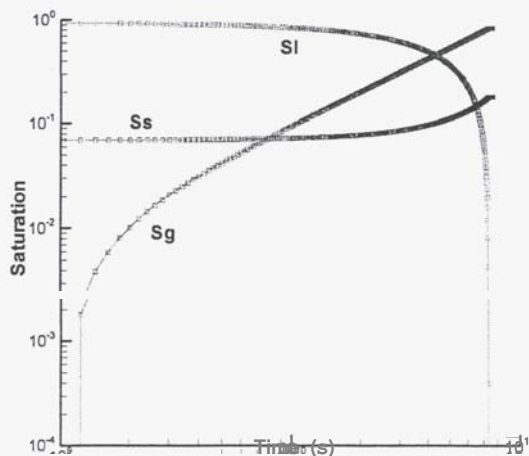


Figure 4. Evolution of liquid, vapour and solid phase saturations for a 1D 'box' of hypersaline fluid, initially at $P = 500$ bar, $T = 550$ °C and $X = 0.5$. Water and salt are added to the box at the rate of 0.1 kg/s each, and fluid is withdrawn at 0.188 kg/s.

3.1-D HORIZONTAL EXAMPLE

In this example NaCl-TOUGH2 is used to demonstrate that multi-phase brine flows in a simple geometry can be handled correctly. The model domain comprises a horizontal 'column' with fluid production from one end and fixed pressure, temperature and salt mass fraction at the other. The domain is 1 kilometre long and is divided into 100 elements. The properties of the rock are: permeability 5×10^{-15} m², porosity 0.01, heat capacity 1000 J/kg/K, thermal conductivity 3 W/m/K and density 2650 kg/m³.

Initially the fluid is in the liquid state with $P = 200$ bar, $T = 350$ °C and $X = 0.3$. The left hand end of the domain is held at these conditions and fluid is withdrawn at the rate of 0.05 kg/s from the right hand end. The simulation continues until the pressure is zero at the right hand end.

As the pressure decreases, fluid in the domain changes from pure liquid (state 1) to two-phase (1+g, state 3), to three phase (1+g+s, state 4) and finally to two-phase (g+s, state 6). These phase changes result in increasing precipitation of solid salt. As the mobile fluid at the withdrawal point turns to low density gas (in state 6) the pressure there falls rapidly. At $t = 0.48 \times 10^7$ the pressure at the withdrawal point has reached almost zero, and it is no longer possible to maintain the extraction of fluid. Figure 5 shows the pressure at that time and Figure 6 shows the corresponding solid, liquid and gas saturations. Figure 7 shows the mass fraction of salt along the domain. This shows that the two-phase (g+s, state 6) 'fluid' is almost completely comprised of solid salt at the end of the simulation.

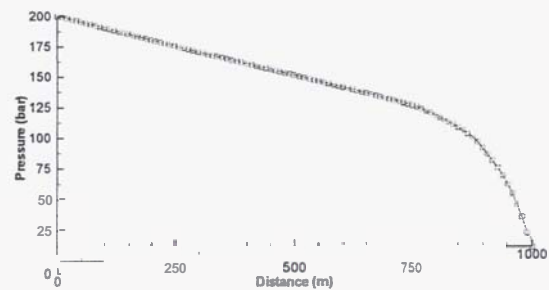


Figure 5. Pressure distribution in a 1D column at the point where precipitation of solid salt and evolution of a gas phase mean that withdrawal from the column is no longer possible.

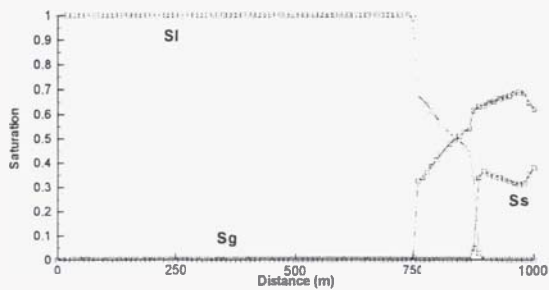
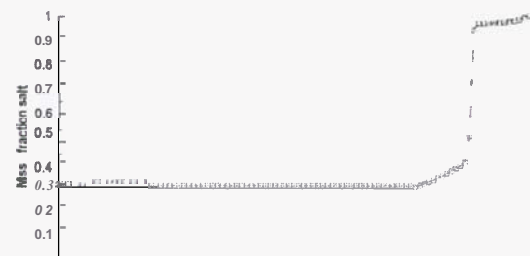


Figure 6. Distribution of liquid, vapour and solid saturations in a 1D column at the point where precipitation of solid salt and evolution of a gas phase mean that withdrawal from the column is no longer possible.



4.2-D CONVECTION

In this section a 2-D TVZ-like example is presented. The model domain is 80 km wide by 8 km deep. Heat, salt and magmatic water are applied over the central 30 km of the model domain at rates of 3000 W, 3×10^{-5} kg/s and 3×10^{-4} kg/s respectively. The permeability of the model domain is 100×10^{-15} m² horizontally, and 10×10^{-15} m² vertically in the upper 2 km above the heat source, and is tenth of this elsewhere.

Figures 8 and 9 show temperature and salinity in this model at 2×10^6 years. The temperature shows two broad, rather unstable plumes. Two

narrow plumes of concentrated brine occur surrounded by diffuse envelopes of lower salinity fluid. The relatively sharp edges of these plumes are caused by inflows of pure water. As the plumes move, the salinity of the fluid can change more rapidly than the temperature, and this results in the front-like behaviour of the salinity.

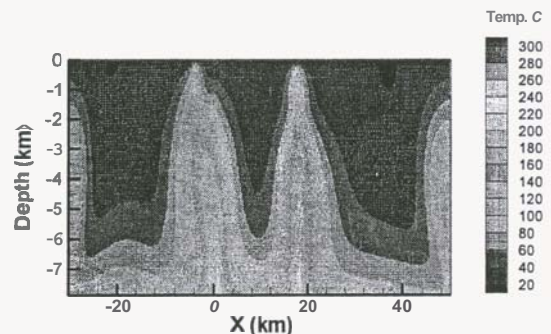


Figure 8. Temperature distribution in a 2D TVZ-like model at 2000000 years. There are two plumes of geothermal fluid. Deeply penetrating flows of cool surface water occur on both sides of, and between, these plumes.

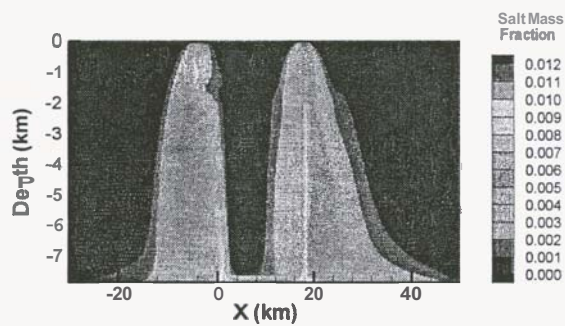


Figure 9. Salt concentration in a 2D TVZ-like model at 2000000 years. Two plumes of saline geothermal fluid are present, with downflows of zero-salinity fluid from the surface occurring in between, and exterior, to the plumes.

5. TWO PHASE TRAVELLING WAVES AND SHOCKS

The last examples presented in this paper concern the motion of travelling saturation waves in a horizontal two phase (liquid + gas) hypersaline system. Understanding the propagation of these waves could find application, for example, in the analysis of well tests in two-phase hypersaline geothermal reservoirs.

The model domain consists of a column 1 m long, divided into 200 elements. The initial pressure, temperature and liquid saturation are 46 bar, 262 °C and 0.4 respectively. Rock properties are: density 2650 kg/m³, porosity 0.3, permeability 10⁻¹⁶ m², heat capacity 1000 J/kg/K. The initial pressure gradient is -1.22 bar/m, implying liquid, gas and heat fluxes of 3.5 × 10⁻⁵ kg/m²/s, 9.2 × 10⁻⁶ kg/m²/s and 65.8 W/m². Heat conduction has been ignored in these examples.

In the first example, the saturation at the upstream end is raised to 0.6. Saturation as a function of time are shown in Figure 10. This shows shock-like waves because the characteristic speed of the upstream side of the wavefront is greater than that on the downstream side. The wavefront remains unchanged throughout the simulation, with a speed of about 0.45×10^{-6} m/s.

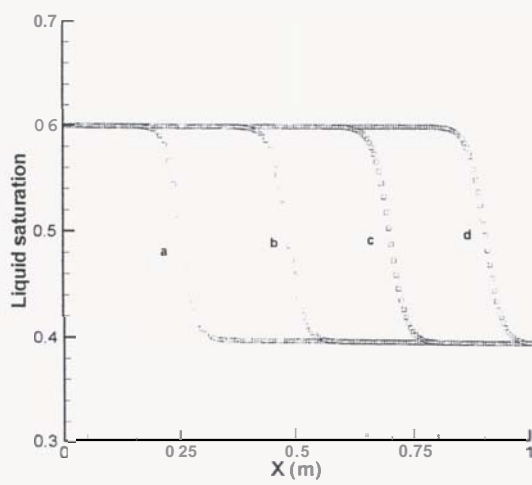


Figure 10. Liquid saturation profiles for first 1-D travelling wave example. The curves a, b, c and d correspond to times of 0.5, 1.0, 1.5 and 2.0×10^6 seconds respectively. The wave takes the form of a shock because wave speed increases with saturation, and the upstream side of the wave 'catches up' with the downstream side.

The pressure for this example is shown in Figure 11. This shows the characteristic 'kinked' pressure profile which occurs in these systems (Kissling *et al.*, 1992). The pressure gradient is discontinuous at the kink.

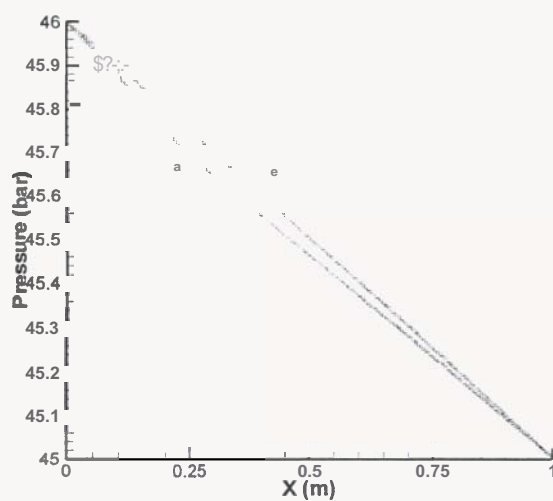


Figure 11. Pressure profiles for first 1-D travelling wave example. The curves a and e correspond to times of 0.5 and 3.0×10^6 seconds respectively. The 'kink' in the curve near the 'a' is the location of the wavefront, where the pressure gradient is discontinuous. For curve e, the wave has passed completely through the domain.

In the second example in this section, the saturation at the upstream boundary is dropped to 0.2. The liquid saturation as a function of time is shown in Figure 12. This shows that the saturation propagates as an expansion fan. This is because the characteristic speed on the upstream side of the wavefront is slower than that on the downstream side. Thus the saturation profiles tends to become more smeared out with time.

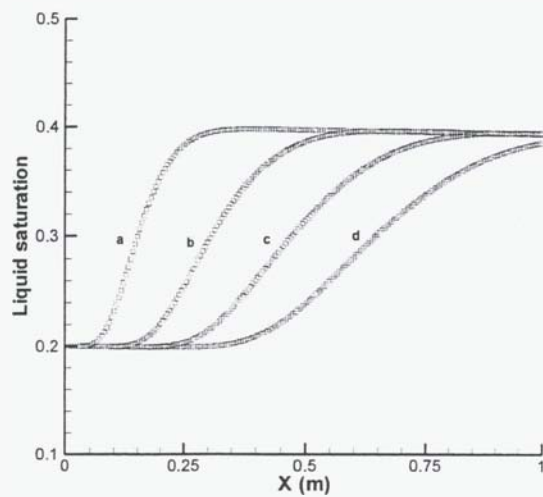


Figure 12. Liquid saturation profiles for second 1-D travelling wave example. The curves a, b, c and d correspond to times of 0.5, 1.0, 1.5 and 2.0×10^6 seconds respectively. The wave takes the form of an expansion fan in this example because the wave speed decreases with decreasing saturation and the upstream end of the wave travels more slowly than the downstream end.

6. CONCLUSIONS

This paper has presented a number of examples in 0, 1 and 2-D settings which demonstrate the application and versatility of NaCl-TOUGH2. In particular, these problems demonstrate the code can handle the flows of high pressure and temperature, high salinity brines in problems where phase changes occur, and also in problems of geophysical interests.

7. REFERENCES

Christenson, B.W., Wood, C.P., Arehart, G.B (1998). Shallow magmatic degassing: Processes and PTX contraints for paleo-fluids associated with the Ngatamariki diorite intrusion, New Zealand. *Water-Rock Interaction* 9, Taupo, 435-438.

Giggenbach, W.F. (1992). Magma Degassing and Mineral Deposition in Hydrothermal Systems along Convergent Plate Boundaries. *Econ. Geol.*, 87, 1000-1014.

Kissling, W.M., McGuinness, M.J., McNabb, A., Weir, G.J., White, S.P., and Young, R.M. (1992). Analysis of One-Dimensional Horizontal Two-Phase Flow in Geothermal Reservoirs. *Transport in Porous Media*, 7, 223-253.

Kissling, W.M. (2000). Progress on a Brine Module for TOUGH2. Proc. 22nd New Zealand Geothermal Workshop, 251-256.

McNabb, A. (1992). The Taupo-Rotorua Hotplate. Proc. 14th New Zealand Geothermal Workshop, 111-114.